

# The Propagation of Pressure in a Gelled Waxy Oil Pipeline as Studied by Particle Imaging Velocimetry

Husam El-Gendy, Mataz Alcoutlabi, Mark Jemmett, Milind Deo, and Jules Magda

Dept. of Chemical Engineering, University of Utah, Salt Lake City, UT 84112

Rama Venkatesan, and Alberto Montes

Chevron Energy Technology Company, Houston, TX 77002

DOI 10.1002/aic.12560

Published online March 2, 2011 in Wiley Online Library (wileyonlinelibrary.com).

*Paraffinic crude oils in pipelines may form waxy gels during flow shutdowns. These gels can be dislodged by applying pressure if the wall shear stress, proportional to the local pressure gradient, exceeds the gel yield stress. The simplest models assume that the axial pressure profile becomes linear immediately after a jump in upstream pressure, but this fails to account for gel time-dependent rheology or the effect of gel voids on pressure wave propagation. To investigate the former factor, pressure profile and particle imaging velocimetry (PIV) measurements were performed on a model oil gelled under pressure to reduce void formation. After a jump in upstream pressure to a value insufficient to restart flow, the axial pressure profile becomes linear in a two-step process, with an immediate small rise in downstream pressure followed by a time-delayed jump. The local downstream gel deformation measured by PIV exhibits similar two-step time dependence.* © 2011 American Institute of Chemical Engineers *AICHE J.*, 58: 302–311, 2012

**Keywords:** energy, petroleum, PIV, rheology

## Introduction

An important problem in the current energy resources market is the need to maintain the flow of waxy crude oils in long pipelines despite their tendency to form gels during shutdown periods. Waxy crude oils comprise about 20% of the world petroleum reserves,<sup>1</sup> and are increasing in importance due to dwindling supplies of oils with lower pour points. After a long shutdown period, a gelled pipeline can usually be restarted by applying pressure on the gel using a pusher fluid, provided that the required pressure does not exceed the maximum allowable pipe pressure. Waxy crude

oils of course vary greatly in composition and in the strength of the gels that they form when cooled below their gelation temperatures. Hence, there is a need for identifying and measuring the appropriate gel properties that can be used for accurate prediction of the minimum pressure required for restarting flow in gelled pipelines. The most obvious choice is the rheological property known as the static yield stress ( $\tau_s$ ), defined as the maximum shear stress that the gel can withstand without fracture or flow.<sup>2</sup> However, measurement of  $\tau_s$  in a laboratory rheometer is of no quantitative significance unless the actual stresses exerted on the gel in the pipeline during flow restart can be calculated. The wall shear stress exerted on the gel at a given axial position  $z$  is related to the local axial pressure gradient ( $-dP/dz$ ), as shown by performing a force balance (Figure 1) on a differential axial element of the gel. The resulting equation is given by:

Correspondence concerning this article should be addressed to J. Magda at jj.magda@m.cc.utah.edu.

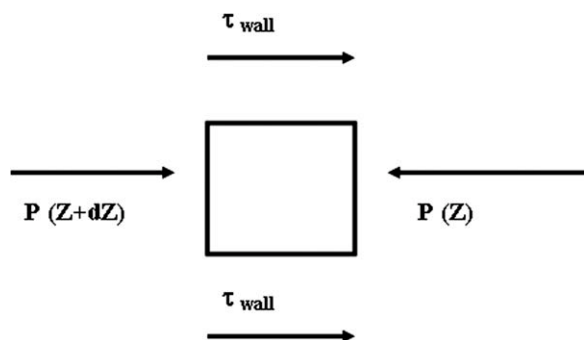


**Figure 1. Force balance on differential axial element of gel in pipeline.**

$$\tau_{\text{wall}} = 0.5 R (-dP/dz) = G\gamma. \quad (1)$$

Here,  $R$  is the inner radius of the pipeline,  $\tau_{\text{wall}}$  is the shear stress exerted on the gel at the wall,  $G$  is the gel shear modulus, and  $\gamma$  is the shear strain deformation of the gel at the wall. Hence, knowledge of the pipeline axial pressure profile and its speed of propagation are of paramount importance to predictions of flow restart. The first gelled pipeline restart models developed assume that the axial pressure profile becomes linear immediately after application of an upstream restart pressure.<sup>3–5</sup> This assumption is based on the following reasoning. Pressure waves are thought to travel at the speed of sound, which approaches infinity inside a gel assumed to be almost incompressible. For a gel that is initially uniform, there is no reason to expect gel deformation at the wall  $\gamma$  or the gel shear modulus  $G$  to vary with axial coordinate  $z$  after pressure propagation is complete (assuming restart has not yet occurred). Therefore, for Eq. 1 to be satisfied after pressure propagation,  $-dP/dz$  must be independent of  $z$ , that is, the axial pressure profile must be linear. Furthermore, the entire length of the gel should fracture simultaneously at a minimum value of the overall pressure gradient given by<sup>3</sup>:

$$\Delta P_{\text{min}} = 2 L \tau_s / R, \quad (2)$$

where  $L$  is the length of the gel. As discussed by Henaut et al.,<sup>6</sup> Eq. 2 is widely believed to be too conservative and overestimates the minimum restart pressure when  $\tau_s$  is obtained via rheometry, leading to pipe overdesign or unnecessary use of chemicals. Possible reasons why Eq. 2 overpredicts the minimum pressure drop needed to restart flow in the pipe include the occurrence of very slow cooling rates in field pipelines, gravity settling of the wax crystals during cooling in large diameter pipes, time-dependent rheology effects, and compressibility effects. In addition, Borghi and Corra<sup>7</sup> have shown experimentally that the pressure profile does not become linear immediately after application of an elevated upstream pressure on a gelled pipeline. To account for these two puzzling observations, a number of authors have proposed newer pipeline restart models in which the gels are assumed to be highly compressible due to the presence of voids formed via shrinkage during gelation. According to these models,<sup>1,8,9</sup> when pressure is applied upstream of the gel,

gel compressibility effects give rise to a slowly propagating compression front with a steep pressure gradient that fractures the structure of the gel that it passes through. Hence, according to these newer models,<sup>1,8,9</sup> the presence of a large volume fraction of voids in the oil after gelation explains both why the pressure profile does not become linear without a delay upon application of an elevated upstream pressure, and why gel fracture occurs at a smaller overall pressure drop than predicted by Eq. 2.

However, void formation due to shrinkage should be greatly reduced if the oil in the pipeline gels at fixed pressure rather than at fixed overall volume. Even in the field, one typically has risers and downcomers connecting to the pipeline; hence, there will almost always be a static head that pressures the liquid during the gelation. In addition, by applying a fixed upstream pressure value during gelation, one can hope to exert better control over the pressure profile present in the gel prior to restart. This is the approach favored in the work presented here. Through a combination of rheology measurements, pressure profile measurements, and particle imaging velocity (PIV) measurements, we investigate the axial pressure profile and the validity of Eq. 2 for a model waxy oil system. As shown in Results, Eq. 2 gives a reasonably accurate prediction of the minimum restart pressure. However, even for our model oil gelled under pressure and ostensibly containing few voids, the axial pressure profile becomes linear in a slow two-step process, with an immediate small rise in downstream pressure followed by a time-delayed jump. We attribute the delayed jump in the downstream pressure to the slow time-dependent rheological relaxation behavior of the shear modulus  $G$ , not to gel compressibility. This is plausible because Eq. 1 relates  $G$  to the pressure drop across a differential gel element, hence the steady-state pressure profile cannot be attained until the value of  $G$  fully relaxes.

## Materials and Methods

### Materials

Model waxy crude oils that are transparent above the wax appearance temperature (WAT) were prepared by dissolving 7 wt % wax (food grade) in Superla mineral oil (specific gravity 0.85, viscosity 20 mPa s at 25°C). To avoid potential evaporation problems, no volatile components such as kerosene were included in the formulation. The carbon number distribution in the added wax peaked at a carbon number of about 30, as measured using high temperature gas chromatography (HP 5890).<sup>10</sup>

### Rheology

Rheological measurements were performed using cone-and-plate fixtures (40 mm diameter, 0.035 radians cone angle) on a controlled-stress rheometer (AR 550 from TA Instruments, Newcastle, DE). Sample temperature and cooling rate were controlled using the rheometer Peltier plate. Because the gap of the cone-plate fixtures is only 48  $\mu\text{m}$ , the model oil studied via rheometry did not contain tracer particles as used in the flow restart experiments. A systematic procedure was followed for preheating the sample above the wax disappearance temperature,

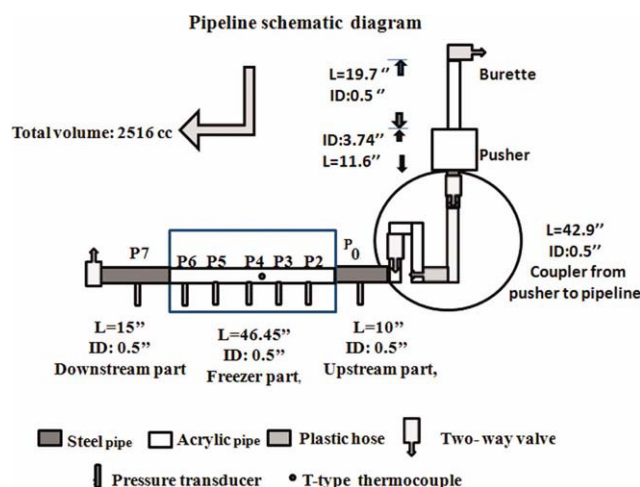


**Figure 2. Schematic diagram of the test section of the laboratory flow loop.**

The model oil is gelled within a transparent section (indicated with a rectangle in the sketch) containing five pressure transducers P2–P6. The flow direction is from right to left. The upstream liquid contains two pressure transducers P0 and P1 that are close enough to overlap on the scale of this sketch. [Color figure can be viewed in the online issue, which is available at [wileyonlinelibrary.com](http://wileyonlinelibrary.com).]

loading it into the rheometer, cooling it and performing tests such as small amplitude oscillatory shear and creep-recovery measurements. The cooling rate was typically 0.1–1.0°C/min, chosen to match the cooling rate used in gelled pipeline flow restart experiments (see below). Small amplitude oscillatory shear measurements were used to obtain the WAT and the gelation temperature, whereas the creep-recovery tests were used to investigate the gel yielding behavior.

### Laboratory flow loop

The gelled restart behavior of the transparent model oils was studied using the Utah Petroleum Research Center laboratory flow loop. Figure 2 shows a schematic diagram of the test section within the flow loop. The key portion is a transparent acrylic pipe section ( $L = 118$  cm,  $R = 0.635$  cm,  $L/R = 186$ ) mounted with one thermocouple (T-type) and five pressure transducers (Omega model PX302-050GV, 50 psi full-scale). The transparent pipe section is enclosed within a clear plastic box which protrudes from a rectangular hole in the top surface of a freezer. The freezer cools the transparent pipe section from 40°C to a steady temperature of about 0°C  $\pm$  2°C after 1 h of cooling. The remainder of the flow loop (except for a heated reservoir not shown in Figure 2) contains the same model oil at room temperature. Hence, the pusher fluid is a non-Newtonian slurry, because the WAT of the model oil is above room temperature. The reservoir tank is equipped with a heating coil which is connected to a water bath, where the temperature of the model oil is controlled. The model oil is heated to about 25°C above the wax appearance temperature in the reservoir, with stirring to melt all wax and remove any thermal history and to obtain a homogenous solution. As shown in Figure 2, the flow loop

contains additional pressure transducers within the liquid, two upstream of the gel, and one downstream of the gel. The pressure transducers and thermocouples are controlled by a National Instruments module which is monitored by a personal computer. Compressed nitrogen gas is used to apply a known and constant pressure on the pusher fluid on the upstream end of the test section. The hydrostatic head from the model oil reservoir contributes an additional upstream pressure of about one psi.

### Particle imaging velocimetry

After the gel fractures, the axial pressure gradient becomes zero because the gel can no longer withstand a shear stress at rest. Thus, the measured axial pressure gradient can be used to detect fracture. In addition, we use Particle Imaging Velocimetry (PIV) to identify the radial location of the fracture. The particle image velocimetry technique<sup>11</sup> was used to monitor the velocity field, and hence displacement, of fluorescent seeding microparticles (0.2% by volume, rhodamine B-marked melamine resin, 10  $\mu$ m mean diameter, density 1500 kg/m<sup>3</sup>, from Fluka) in the gelled part of the pipeline under the applied pressure. The PIV system (Lavision) consists of a PIV camera (Imager ProX4M, Lavision, 2048  $\times$  2048 pixels) and a double-headed Laser unit (NewWave Research, 15 Hz max repetition rate in single mode and 7.5 Hz in double mode, 50 mJ per pulse) in addition to the programmable timing unit PTU (Lavision) which controls the timings of the lasers and the camera. The time between the two lasers is 68 ms and the cross correlation method was used in the computation of the velocity flow field, with interrogation window size of 64  $\times$  64 pixels with 50% overlapping. The laser beam was transformed into a laser sheet by using a combination of spherical and cylindrical lenses. The laser sheet passes through the center of the pipeline such that the sheet, the flow and the camera are perpendicular to each other (see Figure 3). Figure 4 shows an example of the velocity field obtained by PIV for the Newtonian mineral oil. As expected, the velocity field is parabolic, but with a slight downward tilt due to the density mismatch between the seeding particles and the low viscosity mineral oil. The field-of-view of the CCD camera is 2.0 cm by 1.25 cm, with a resolution in particle displacement measurement of order 10  $\mu$ m. Given that we only have one camera, repeat experiments are necessary in order to compare the gel deformation at axial positions separated by more than 2 cm.

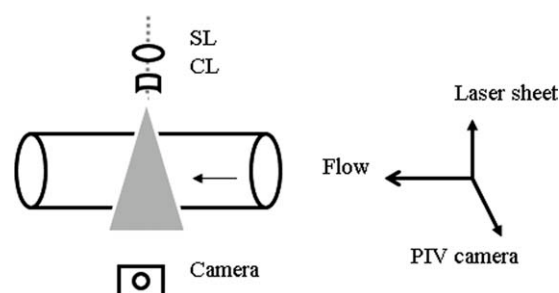


**Figure 3. Geometry of PIV laser sheet used to monitor displacement of gel in pipeline.**

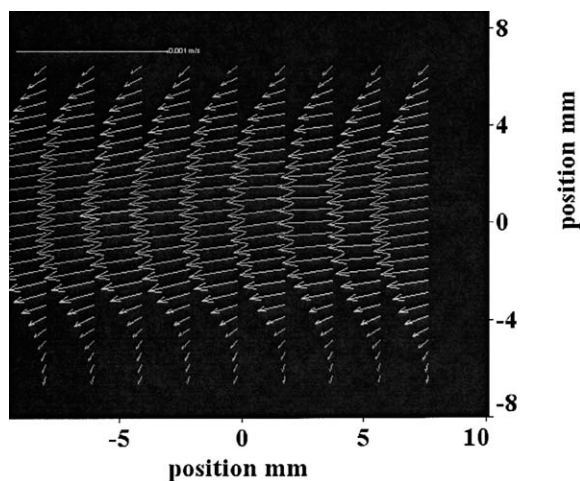


**Figure 4. Velocity field of Newtonian mineral oil in laboratory pipeline obtained by PIV.**

The maximum duration of PIV measurements is  $\sim 720$  s due to computer storage limitations.

#### **Gelation and flow restart procedure**

First the model oil was heated to  $55^{\circ}\text{C}$  in the reservoir and circulated through the flow loop several times to ensure a homogenous distribution of PIV tracer particles. The temperature of the oil cools to about  $40^{\circ}\text{C}$  as it travels from the reservoir to the test section. Then the pump was stopped, the downstream valve was closed, and the freezer was used to cool the transparent test section. In some cases, compressed nitrogen was used to exert a constant upstream pressure on the oil within the transparent test section during gelation. Eight pressure transducers were used to monitor the axial pressure profile during gelation. After a predetermined cooling time, the enclosure around the pipeline test section was quickly removed and the pressure data acquisition software program was restarted. Approximately 10 s later, compressed nitrogen gas was used to suddenly increase the upstream pressure value and the PIV image acquisition software program was started. All flow restart data in this work were obtained with the downstream valve closed so that a constant upstream pressure on the oil within the transparent test section could be applied during gelation. Because shear deformation of the material occurs with negligible volume change, the closed downstream valve does not prevent initial gel fracture, though it will likely affect the clear out time for the gel.

## **Results**

### **Rheology**

The rheological behavior of the model oil containing 5 wt % added wax has been presented in an earlier publication.<sup>10</sup> There, it was shown that both the WAT and the gelation temperature can be determined by performing small amplitude shear oscillations (frequency =  $0.126$  rad/s, stress amplitude =  $0.3$  Pa) while cooling the model oil from high temperatures at  $0.1^{\circ}\text{C}/\text{min}$ . In such an experiment, the WAT is identified with the departure of the viscosity temperature

dependence from Arrhenius behavior, and the gelation temperature is identified with the temperature at which the shear elastic modulus first exceeds the shear viscous modulus.<sup>10</sup> The same experimental approach was applied to the model oil containing 7 wt % added wax. To summarize, we find that the WAT is  $29^{\circ}\text{C}$  when the model oil contains 7 wt % added wax, and the gelation temperature is  $27^{\circ}\text{C}$  (uncertainty  $\pm 0.5^{\circ}\text{C}$ ). The closeness of the WAT and the gelation temperature for this model oil probably reflects the carbon number distribution in the added wax, which is narrower than is typical for crude oils.

Time-dependent yielding behavior was also reported for the model oil with 5 wt % added wax in Reference 10. Following Chang et al.,<sup>2</sup> we define two yield stresses for the waxy gels: the elastic-limit yield stress value  $\tau_e$ , and the static yield shear stress value  $\tau_s$ . If the shear stress imposed on a waxy oil gel is below  $\tau_e$ , then the gel only exhibits reversible elastic behavior without creep. If the shear stress imposed on the same gel is above  $\tau_s$ , then the gel fractures and flows. If a shear stress intermediate between  $\tau_e$  and  $\tau_s$  is imposed, then the gel slowly creeps and may eventually fracture given sufficient time. Thus the precise value of  $\tau_s$  depends on the duration of the experiment or on the rate-of-stress loading on the wax gel, a phenomenon reported for gels formed from both model oils<sup>10</sup> and waxy crude oils.<sup>2,6,12</sup> This type of behavior is shown by results given in Figure 5 for a creep test at  $2^{\circ}\text{C}$  on the model oil with 7 wt % added wax. At time equal zero, a constant shear stress  $\tau$  of  $160$  Pa was suddenly imposed on the gel sample using a cone-plate rheometer. As observed in Figure 5, the value of the shear strain  $\gamma$  increases with time as the gel creeps. Thus, the value of the shear modulus  $G = \tau/\gamma$  does not reach a steady value over the duration of the experiment. For a creep experiment at a higher stress level ( $240$  Pa) on the same sample, one observes in Figure 5 that gel fracture occurs after a short delay time of  $1$ – $2$  s. We arbitrarily chose an observation time of  $1$  min in the creep tests performed to determine  $\tau_e$  and  $\tau_s$  values. To summarize the creep test results, we find that  $\tau_e$  is  $70$  Pa and  $\tau_s$  is  $200$  Pa for the model oil containing 7 wt % added wax (uncertainty  $\pm 40$

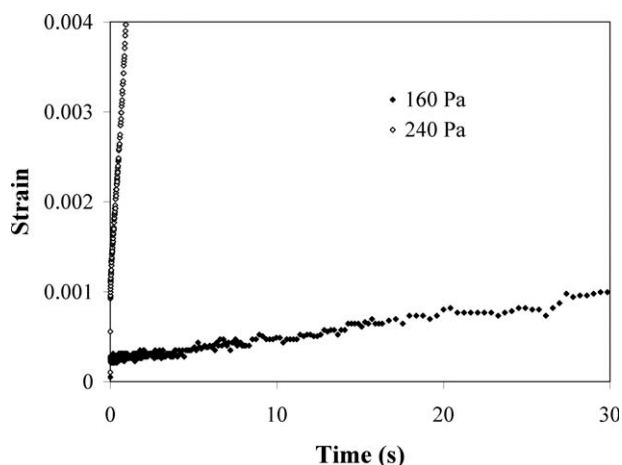


**Figure 5. Time-dependent shear strain of model oil gel at  $2^{\circ}\text{C}$  subjected to the constant cone-plate shear stress values given in the legend.**



Pa) at 2°C. Substituting these stress values into Eq. 2, one calculates overall pressure drops across the gel of 4 psig and 11 psig, respectively, provided the assumptions of Eq. 2 are satisfied, such as that of a linear axial pressure profile.

### Pressure profiles during gelation

Because the density of a crude oil increases as it gels, several authors have suggested that waxy gels that form within pipelines may contain numerous voids that profoundly affect the compressibility and restart behavior of the gel.<sup>1,6,8,9</sup> As discussed in the Introduction, gel compressibility due to voids is thought to be responsible for a delay in the time at which the axial pressure profile reaches steady state, as well as a minimum restart pressure smaller than predicted by Eq. 2. To reduce gel void volume fraction, and also to control the pressure profile present in the gel prior to restart, the waxy oil was pressurized during gelation. In these experiments, a constant nitrogen pressure was applied to the upstream end of the transparent test section (Figure 2) with the downstream valve closed. Figure 6 shows the results obtained for the time-dependent pressure during cooling of the waxy model oil (7% added wax) for 1 h under a constant upstream pressure of 12 psig with the downstream valve closed. This is an upstream pressure value that is sufficient to dislodge gels which have been formed at ambient pressure with the downstream valve open. During the hour of cooling, the temperature recorded by the thermocouple (for location, see Figure 2) decreased from 40°C to 0°C. Hence, the initial gel temperature was above the WAT (29°C), and the final temperature was well below the gelation temperature (27°C). The signal from all five pressure transducers located within the gel (P2–P6) drops monotonically with cooling time, whereas the signal from the two transducers in the liquid upstream of the gel (P0 and P1) remains constant at ~12 psig (82.7 kPa). Furthermore, the pressure measured by the transducer in the liquid downstream of the gel (P7) also decreases with cooling time. Hence, there can be no question that gel formation attenuates the magnitude of the pressure reaching the closed downstream valve, as measured by the transducer labeled P7 in Figure 2. At lower values of upstream pressurization during gelation (<5 psig), the pressure measured by transducer P7 decreases from the upstream pressure value to the ambient pressure value (zero psig) during the gelation process. Consider an axial force balance on the oil upstream of the closed valve, including that in the test section. Prior to gelation, the force arising from the elevated upstream pressure is balanced solely by the force exerted by the closed downstream valve. After gelation, the force arising from the elevated upstream pressure is balanced solely by the shear stress exerted by the pipe walls. The qualitative explanation is simple. As the waxy oil cools, it contracts and moves downstream away from the applied nitrogen pressure. At some point in time, the oil gels and adheres to the pipe wall. As the gel contracts further, it experiences a shear strain as it continues to adhere to the wall. By definition, a gel can resist a shear stress at rest. Thus subsequently the upstream pressure is attenuated by the shear stress exerted by the pipe walls on the gel ( $\tau_{\text{wall}}$ ), in accordance with Eq. 1 and Figure 1. Quantitative prediction of the axial pressure profile after gelation is complete is

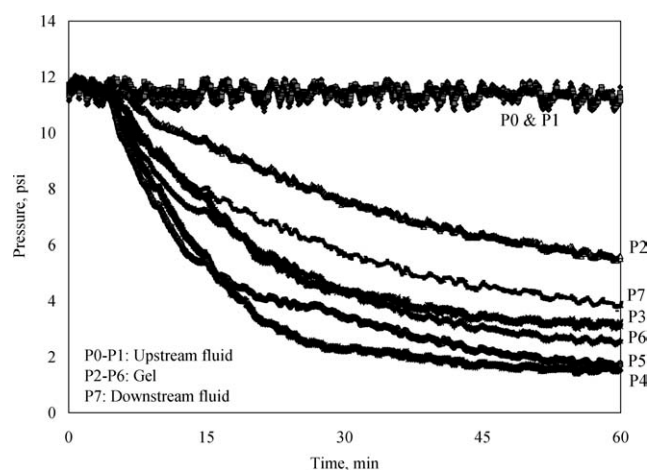


**Figure 6. Pressure vs. time measured by eight pressure transducers within flow loop as waxy oil is cooled from liquid to gel under applied upstream pressure of 12 psig (82.7 kPa).**

Transducers P0 and P1 are in the liquid upstream of the gel and P7 is in the liquid downstream of the gel (see Figure 2).

quite difficult, as  $\tau_{\text{wall}}$  must depend on factors such as the degree of wall adhesion, the coefficient of thermal contraction, the density change upon gelation, and the gel shear modulus. Furthermore, one notices in Figure 6 that the pressure value after 1 h of cooling does not decrease monotonically with pipe axial position  $z$ , probably due to nonuniform cooling. Hence, neither the pressure nor the wall shear stress is uniform within the gel prior to restart, as commonly supposed in most restart model calculations.<sup>5,8</sup> The nonuniform deformation or residual stresses present in the gel after cooling may profoundly affect the minimum restart pressure, a hypothesis that we will address in future research.

### Time-dependent pressure profile and PIV after application of restart pressure

**Unsuccessful Restart.** In a series of restart tests, the model oil (7 wt % added wax) was gelled by cooling for 4.5 h under an upstream pressure of 1 psig (6900 Pa) (i.e., the hydrostatic head of the oil reservoir), and then subjected to a sudden increase in upstream pressure to  $P_{\text{in}}$ . The temperature of the model oil, initially 40°C, dropped to about 0°C in about 1 h. Hence, the gel was aged at 0°C for about 3.5 h prior to the restart attempt. We found that a jump in upstream pressure value from 1 psig (6900 Pa) during cooling to  $P_{\text{in}} = 5$  psig (34.5 kPa) was insufficient to restart the flow, at least within 12 min, as shown by the results in Figure 7. If the gel fractures and releases from the wall,  $\tau_{\text{wall}}$  becomes zero and the axial pressure gradient must be zero (see Eq. 1). This is clearly never the case in Figure 7, hence we conclude that an upstream pressure value of 5 psig (34.5 kPa) is insufficient to fracture the gel cooled at 1 psig (6900 Pa). The axial pressure profile within the gel keeps evolving in Figure 7 and has not reached a steady state even after 12 min. This result contradicts the assumption of some restart models that the gel axial pressure profile becomes linear immediately after application of an elevated upstream pressure value.<sup>3–5</sup> One might be

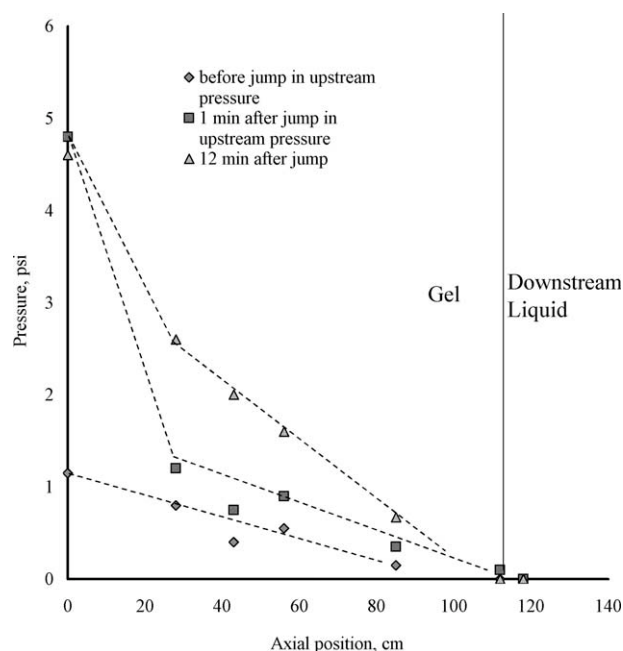


**Figure 7. Pressure vs. axial position measured from the upstream liquid/gel interface at the times given in the legend.**

The gel was cooled for 4.5 h at an upstream pressure value of 1 psig (6.9 kPa), and then the upstream pressure was suddenly increased to 5 psig (34.5 kPa). The presence of a non-zero axial pressure gradient at all experimental times indicates that the gel did not fracture.

tempted to say that the propagation time of the compression front is very slow,<sup>1,8,9</sup> of order 12 min here. However, this is also incorrect, because the downstream gel responds immediately to the jump in upstream pressure value, as shown in Figure 8. As seen in Figure 8a, the pressure at a downstream location begins to increase almost immediately after the jump in the upstream pressure value from 1 psig (6.9 kPa) to 5 psig (34.5 kPa), albeit by a small amount. PIV measurements of the downstream gel (Figure 8b) confirm that the downstream gel displacement responds to the increase in upstream pressure from 1 psig to 5 psig almost immediately. Thus, the pressure propagates through the gel in two steps, not as a single slow-moving pressure front that fractures the gel as it passes through, as predicted to occur in gels containing numerous voids.<sup>1,8,9</sup> The first step is probably associated with the initial propagation of the pressure wave, possibly through the liquid trapped within the porous gel network. The slowness of the second step in the downstream pressure rise is not attributable to slow pressure wave propagation, but can probably be attributed to a slow time-dependent decrease in gel shear modulus  $G$  and  $\tau_{\text{wall}}$ . This slow decrease is reminiscent of the slow “creep” of the same gel that we observe in the cone-plate rheometer (Figure 5 and Reference 10).

According to the results in Figure 7, after a jump in upstream pressure from 1 psig (6.9 kPa) to 5 psig (34.5 kPa), there is a delay of at least 12 min in establishment of the steady-state pressure profile within the gel. A portion of this delay is possibly associated with the slow response characteristics of the pressure transducers themselves when in contact with gel. However, there is little or no delay associ-

ated with the pressure transducers themselves when in contact with liquid. This is shown by the observation in Figure 7 that at time equal 1 min (i.e., the time of the first measurement), the pressure in the upstream liquid (axial position equal zero) has already jumped from 1 psig (6.9 kPa) to 5 psig (34.5 kPa). Our flowloop also has a pressure transducer (P7) in contact with liquid downstream of the gel (Figure 2). Unfortunately, in Figure 7 this transducer does not exhibit any response to the jump in upstream pressure at any time, hence the data of Figure 7 cannot be used to investigate the pressure response in the downstream liquid. This occurred because the final upstream pressure value was relatively small (5 psig), hence the gel itself was able to completely

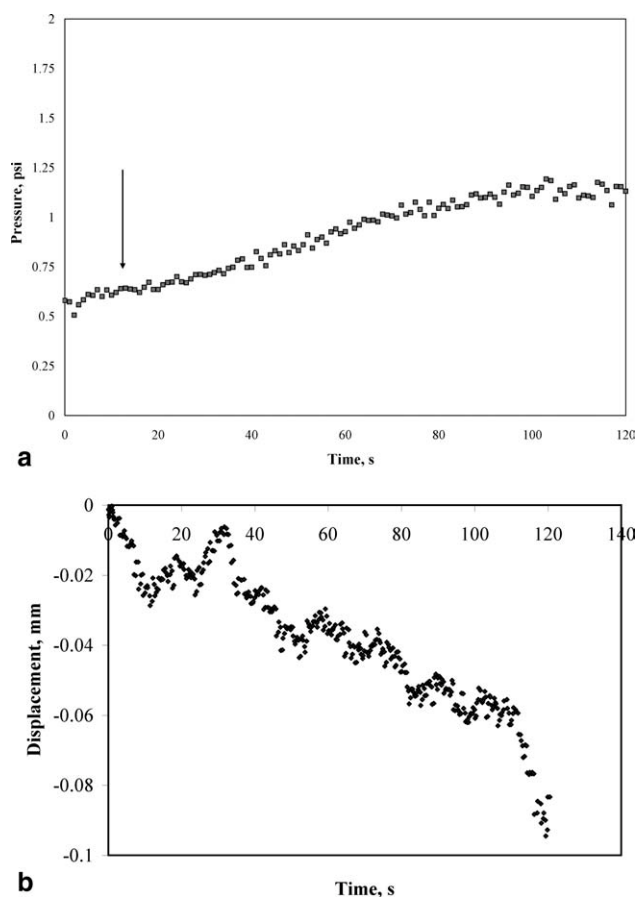


**Figure 8. (a) For the same gel as in Figure 7, short-time response of the pressure in the gel at a location 57 cm downstream from the point of application of the attempted restart pressure; the pressure upstream of the gel was suddenly increased from 1 psig (6.9 kPa) to 5 psig (34.5 kPa) at the time indicated by the arrow; (b) for the same gel as in Figure 7, the short-time gel displacement at the pipe centerline at a location 57 cm downstream from the point of application of the upstream pusher fluid pressure.**

The pusher fluid upstream pressure value was suddenly increased from 1 psig (6.9 kPa) to 5 psig (34.5 kPa) at time equal zero.

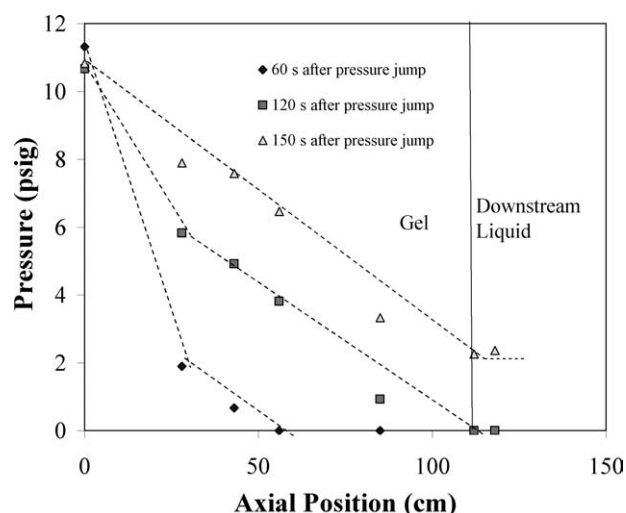


**Figure 9. Pressure vs. axial position measured from the upstream gel-liquid interface at the times given in the legend.**

The gel was cooled for 1 h at an upstream pressure value of 5 psig (34.5 kPa), and then the upstream pressure suddenly increases to 11 psig (76 kPa) at time equal zero.

balance the axial force arising from the jump in the upstream pressure value. In order to investigate the pressure response in the downstream liquid, we must jump to a higher upstream pressure value, as shown by the results in Figure 9. After 4.5 h of gelation at 0°C, the upstream pressure value was suddenly increased from 5 psig (34.5 kPa) to 11 psig (76 kPa). The behavior of the pressure profile during this experiment is shown in Figure 9. The jump in upstream pressure to 11 psig (76 kPa) is seen to be insufficient to fracture the gel within 150 s, since the axial pressure gradient is never zero. As shown in the next section, this gel appears to be stronger than a gel cooled at 1 psig (6.9 kPa) upstream pressure, perhaps because of smaller void volume fraction or perhaps because the model oil was subjected to a relatively high shear stress during gelation. The gel static yield stress value has been shown to increase with imposed shear stress during gelation.<sup>13</sup> One observes in Figure 9 that at time equal one min, the pressure transducers in the upstream liquid (axial position equal zero) give a signal that has already jumped from 5 psig (34.5 kPa) to 11 psig (76 kPa). However, one also observes that the pressure transducer in contact with downstream liquid (axial position equal 120 cm) gives a signal that takes between 120 s and 150 s to increase from zero to a nonzero value of about 2 psig (13.8 kPa). Hence it really does take of order 2–3 min for the full steady-state effect of the jump in upstream pressure (5 psig to 11 psig) to be felt downstream of the gel; this is not an artifact of the transducers when in contact with gels.

**Delayed Restart.** We have seen that a jump in upstream pressure to 5 psig (34.5 kPa) is insufficient to fracture and restart flow of a gel cooled for 4.5 h at 1 psig (6.9 kPa) and ~0°C. However, a gel formed under the same conditions fractures immediately when subjected to a jump in upstream pressure to 12 psig (82.7 kPa), as detected by a rapid increase in pressure downstream of the gel. For the same gelation conditions, Figure 10 shows the dependence of the

fracture time on the upstream pressure value used for attempted restart. For each data point in Figure 10, the model oil was cooled for 4.5 h at 0°C at an upstream pressure value of 1 psig, and then the upstream pressure was suddenly increased to the value plotted on the abscissa. Since the axial pressure gradient becomes zero (Eq. 1) after gel fracture, we define the fracture time as the time at which the response of the last pressure transducer within the gel reaches 80% of the upstream pressure value. Note that if no fracture occurred over the duration of the experiment (720 s), which is the case for jumps in the upstream pressure to values below 8 psig (55 kPa), we define the fracture time to be 720 s in Figure 10. If one assumes a linear pressure profile and uses Eq. 2 in conjunction with the measured gel rheology properties  $\tau_c$  and  $\tau_s$ , then one calculates critical restart pressure values of 4 psig (27.6 kPa) and 11 psig (76 kPa), respectively. The experimentally determined critical restart pressure in Figure 10 is in the range 7–10 psig (48–69 kPa), which is surprisingly close to that predicted by Eq. 2, given that the pressure profile is not linear. For a jump in upstream pressure value from 1 psig (6.9 kPa) to 10 psig (69 kPa), fracture occurs after a delay of 60 s. Figure 11 shows the response of the pressure transducers during this delayed restart experiment. The pressure transducers in the upstream liquid respond almost immediately to the jump in pusher fluid pressure at time equal 8 s, confirming that the inherent response time of the pressure transducers is negligible when in contact with liquid. The pressure is uniform ( $dP/dz = 0$ ) in the pusher fluid, since a liquid cannot resist a shear stress at rest ( $\tau_{\text{wall}} = 0$  in Eq. 1). Hence, transducers P0 and P1 register the same pressure (10 psig) at all times. As the gel fractures away from the wall,  $\tau_{\text{wall}}$  decreases to zero and the pressure rises to 10 psig. One observes in Figure 11 that this occurs sequentially, with fracture occurring first at pressure transducer P2 then later downstream at the location of

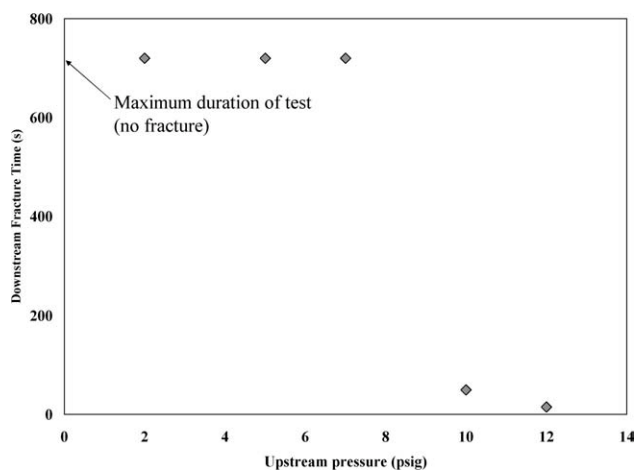


**Figure 10. Fracture time of downstream gel as a function of upstream pusher fluid pressure value.**

For each data point, the model oil was gelled by cooling for 4.5 h at 0°C under an upstream pressure value of 1 psig (6.9 kPa). Note: For upstream pressures less than or equal to 8 psig (55 kPa), the gel did not fracture over the maximum duration of the experiment.

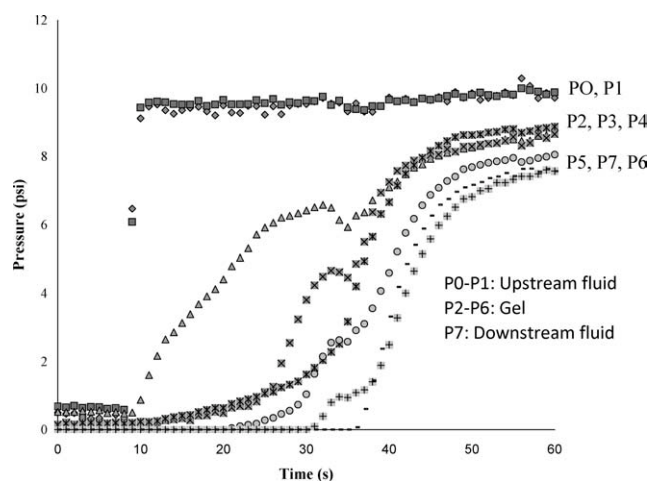


**Figure 11.** Pressure vs. time measured by the eight pressure transducers in the flow loop (see Figure 2 for relative positions).

The gel was cooled for 4.5 h at 0°C with an upstream pressure value of 1 psig (6.9 kPa), and at time equal zero the upstream pressure value was suddenly increased to 10 psig (69 kPa).

pressure transducer P6. During the delayed restart, Figure 12 provides a more detailed look at the response of pressure transducer P4, and Figure 13 shows the time-dependent gel displacement at a location near P4. Figures 12 and 13 both show that there are two distinct times in the restart: the time at which the gel first responds (shown in figure inset) and the time at which fracture occurs. This demonstrates once again that the downstream pressure rise is a two-step process. For the same restart experiment, Figure 14 shows the velocity profile near the wall obtained by PIV  $\sim 30$  s after the jump in the upstream pressure at the axial position of pressure transducer 4. The PIV results, unlike the corresponding pressure profile results (Figure 11), clearly show that the gel has already fractured. The large velocity gradient

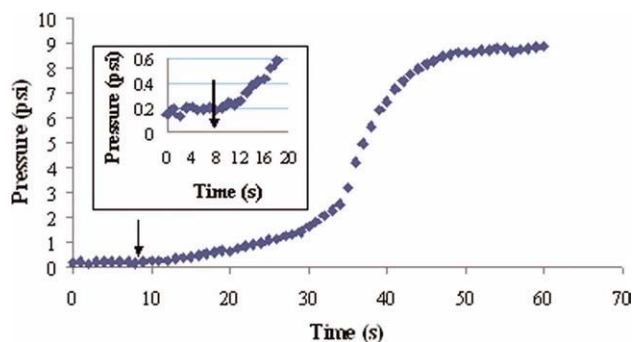


**Figure 12.** For the same gel as in Figure 11, the time-dependent response of pressure transducer four following the jump in upstream pressure from 1 psig (6.9 kPa) to 10 psig (69 kPa) at the time indicated by the vertical arrow.

The short-time behavior is shown in the figure inset. [Color figure can be viewed in the online issue, which is available at [wileyonlinelibrary.com](http://wileyonlinelibrary.com).]

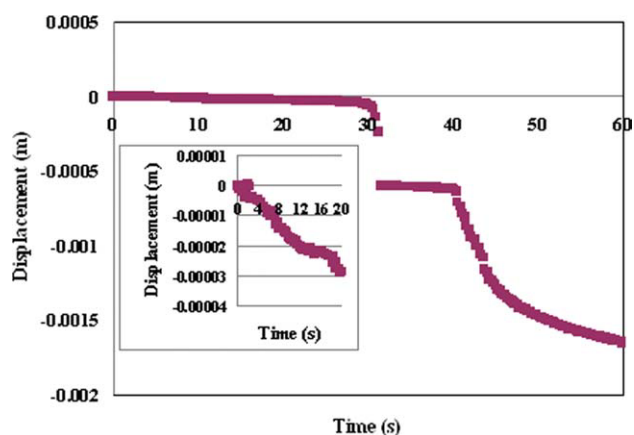


**Figure 13.** For the same gel as in Figure 11, the time-dependent response of the gel centerline displacement at the location of pressure transducer four following a jump in upstream pressure from 1 psig (6.9 kPa) to 10 psig (69 kPa) at time equal zero.

The short-time behavior is shown in the figure inset. [Color figure can be viewed in the online issue, which is available at [wileyonlinelibrary.com](http://wileyonlinelibrary.com).]

observed near the location of the pipe wall in Figure 14 implies that gel fractured first near the wall, where the force balance predicts that the shear stress exerted on the gel is the largest.<sup>3</sup> Moving away from the wall, the axial velocity in Figure 14 becomes approximately constant in value, implying plug-like flow after wall fracture. This is the expected effect of a shear-thinning viscosity value for the fractured gel, and the presence of unfractured material near the centerline where the shear stress approaches zero.

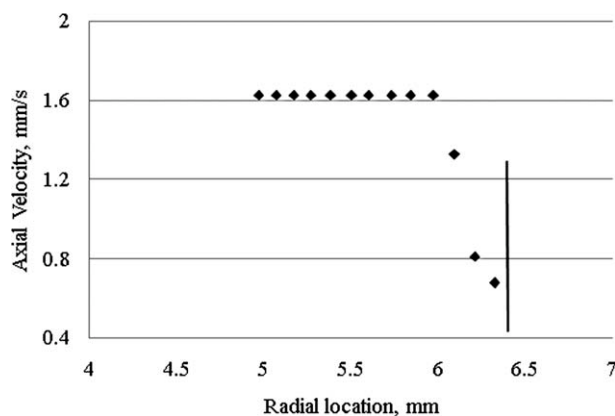


**Figure 14.** For the same gel as in Figure 11, the axial velocity as a function of radial position measured by PIV at the axial location of pressure transducer four thirty seconds following a jump in upstream pressure from 1 psig (6.9 kPa) to 10 psig (69 kPa).

The position of the wall is given by the vertical line. For each point, the average velocity was calculated within a volume having length 5 mm in the axial direction and thickness 0.16 mm in the radial direction.



## Discussion

In this study, we have applied a constant elevated upstream pressure value on a transparent model oil as it was cooled in a pipeline to control the pressure profile present in the gel prior to restart attempts, and to reduce gel void fraction and gel compressibility. Under these conditions, Eq. 2 could be used to predict, within reasonable accuracy ( $\approx 20\%$ ), the minimum pressure required for restart of flow in the pipeline (Figure 10). However, despite the pressurization during cooling, we still observe a considerable delay in the time necessary for the gel to achieve a steady-state linear pressure profile prior to fracture. One must distinguish between two delay times: the time necessary for propagation of the initial pressure wave ( $< 1$  s in Figure 8a), and the time needed for the pipeline pressure profile to reach steady state ( $> 12$  min in Figure 7). For purely viscous liquids, both of these times are very small, but purely viscous liquids, unlike gels, do not exert a shear stress on the pipeline wall at rest (Eq. 1). The first delay time can be attributed to the time necessary for propagation of the initial pressure wave, perhaps through the liquid trapped within the porous gel network. The second delay time is probably related to the slow rearrangement of the gel network under stress. According to Eq. 1, the differential axial pressure drop in the gelled pipeline depends on the gel shear modulus  $G$ . Figure 5 shows that it takes a very long time for  $G$  to reach steady state when subjected to a time-independent shear stress in the rheometer, presumably because long-time rearrangements occur within the gel under stress. We postulate that the same type of long-time rearrangements must occur for the gel within the pipeline before the steady-state pressure profile is obtained. The relaxation of  $G$  first occurs in the upstream gel, because this is where the full value of the shear stress that drives long-time rearrangements is first felt. The full stress value is not experienced by downstream gel until relaxation is complete within the upstream gel. This gives rise to a piece-wise linear pressure profile similar to that assumed to be present in the model of Lee et al.<sup>14</sup> for a different experimental condition, namely restart at constant pusher fluid flow rate. Thus when fracture occurs, the entire gel does not fracture simultaneously, but rather fracture occurs sequentially from upstream to downstream. Hence,  $-dP/dz$  in Eq. 1 is a viscoelastic quantity, with a relaxation time in Figure 7 comparable to that of the creep shear strain seen in cone-plate tests on the same gel (Figure 5). We see additional similarities between the gel cone-plate rheology and the gelled pipeline restart behavior. For example, the pipe flow restarts immediately if the imposed pressure is large, not at all if the imposed pressure is low, and shows delayed restart when the imposed pressure is near the critical value (Figure 10). In cone-plate creep tests,<sup>10</sup> the gel strain exhibits a similar dependence on the imposed shear stress, with delayed fracture observed only near the critical stress value.

The significance of this finding with respect to full-scale operations involving flow assurance and gelled pipeline restart is the following. Even when compressibility effects are minimized, the slow time-dependent creep rheology of waxy oil gels can give rise to a considerable delay in the time needed to attain the steady-state pressure profile after a jump in upstream pusher fluid pressure. This slow time-dependent creep rheology that has been demonstrated here for a single model waxy oil has also been demonstrated pre-

viously for more realistic waxy oils in cone-plate rheology tests, including crude oils.<sup>2,6,10,12</sup>

## Conclusions

If one attempts to control the initial condition of a waxy oil gel prior to flow restart by applying a constant elevated upstream pressure on the oil as it cools, one finds that the downstream pressure value approaches zero in a complicated time-dependent fashion as the oil gels and adheres to the pipe wall. After gelation, if one suddenly increases the upstream pressure to a value that is insufficient to restart flow, the axial pressure profile becomes linear in a two-step process, with an immediate small rise in downstream pressure followed by a time-delayed jump. The local downstream gel deformation measured by PIV exhibits similar two-step time dependence. The first step is probably associated with the initial propagation of the pressure wave, possible through the liquid trapped within the porous gel network. The second step in the downstream pressure rise is most likely related to time-dependent relaxation of the gel shear modulus.

A critical pusher fluid pressure exists for restart of flow in the gelled pipeline. This critical pusher fluid pressure value can be estimated reasonably well using cone-plate rheology yield stress measurements, and assuming a linear pressure profile, at least for model oils gelled under slightly elevated pressure values in the laboratory flowloop. Delayed restart is observed when the pusher fluid pressure is slightly below the critical value. It seems to be possible to estimate the critical restart pressure using the rheology-measured yield stress value, even though there is a delay in time before the pipe pressure profile becomes linear, because this delay time becomes smaller as the pusher fluid pressure approaches the critical restart value. The measured yield stress value cannot be used to estimate the fracture time of the gel in the pipe, and we are investigating other properties, such as the time-dependent slope of the shear creep curve, that might be more useful for this (see Figure 5). When flow restart occurs, the gel fractures first near the pipe wall and sequentially from the upstream end to the downstream end.

## Acknowledgments

Acknowledgment is made by M. A. and J. M. to the donors of the American Chemical Society Petroleum Research Fund (Grant: 45968-AC9).

## Literature Cited

1. Vinay G, Wachs A, Frigaard I. Start-up transients and efficient computation of isothermal waxy crude oil flows. *J Non-Newtonian Fluid Mech.* 2007;143:141–156.
2. Chang C, Boger DV, Nguyen QD. The yielding of waxy crude oils. *Ind Eng Chem Res.* 1998;37:1551–1559.
3. Perkins TK, Turner JB. Starting behavior of gathering lines and pipelines filled with gelled prudhoe bay oil. *J Petroleum Tech.* 1971;301–308.
4. Davenport TC, Somper RSH. The yield value and breakdown of crude oil gels. *J Inst Petroleum.* 1971;57:86–105.
5. Chang C, Nguyen QD, Ronningsen HP. Isothermal start-up of pipeline transporting waxy crude oil. *J Non-Newtonian Fluid Mech.* 1999;87:127–154.
6. Henaut I, Vincke O, Brucy F. *Waxy Oil Restart: Mechanical Properties of Gelled Oils*. Paper SPE 56771 presented at the 1999 SPE Annual Technical Conference and Exhibition, Houston.

7. Borghi GP, Corra S. *Prediction and Scaleup of Waxy Oil Restart Behavior*. SPE. SPE 80259. In International Symposium on Oilfield Chemistry, Houston, Texas. 2003:1–5.
8. Davidson MR, Nguyen QD, Chang C, Ronningsen HP. A model for restart of a pipeline with compressible gelled waxy crude oil. *J Non-Newtonian Fluid Mech.* 2004;123:269–280.
9. Vinay G, Wachs A, Agassant J-F. Numerical simulation of weakly compressible Bingham flows: the restart of pipeline flows of waxy crude oils. *J Non-Newtonian Fluid Mech.* 2006;136:93–105.
10. Magda JJ, El-Gendy H, Oh K, Deo MD, Montesi A, Venkatesan R. Time-dependent rheology of a model waxy crude oil with relevance to gelled pipeline restart. *Energy Fuels.* 2009;23:1311–1315.
11. Grant I. Particle image velocimetry: a review. *Proc Inst Mech Eng Part C.* 1997;211:55–76.
12. Ronningsen HP. Rheological behavior of gelled, waxy North Sea crude oils. *J Petroleum Sci Eng.* 1992;7:177–213.
13. Venkatesan R, Nagarajan NR, Paso K, Yi YB, Sastry AM, Fogler HS. The strength of paraffinic gels formed under static and flow conditions. *Chem Eng Sci.* 2005;60:3587–3598.
14. Lee HS, Singh P, Thomason WH, Fogler HS. Waxy oil gel breaking mechanisms: adhesive vs. cohesive failure. *Energy Fuels.* 2008; 22:480–487.

*Manuscript received May 18, 2010, and revision received Jan. 2, 2011.*